

# Anomalous $tq\gamma$ couplings in $\gamma p$ collision at the LHC

M. Köksal\* and S. C. İnan†

*Department of Physics, Cumhuriyet University, 58140, Sivas, Turkey*

## Abstract

In this work, we have examined the constraints on the anomalous  $tq\gamma$  ( $q = u, c$ ) couplings through the process  $pp \rightarrow p\gamma p \rightarrow pWbX$  at the LHC by considering three forward detector acceptances:  $0.0015 < \xi < 0.5$ ,  $0.0015 < \xi < 0.15$  and  $0.1 < \xi < 0.5$ . The sensitivity bounds on the anomalous couplings have been obtained at the 95% confidence level in a model independent effective lagrangian approach. We have found that the bounds on these couplings can be highly improved compared to current experimental bounds.

---

\*mkoksal@cumhuriyet.edu.tr

†sceminan@cumhuriyet.edu.tr

## I. INTRODUCTION

The top quark is the heaviest particle of the Standard Model (SM). Therefore, the top quark properties, and their production process provide a possibility for probing new physics beyond the SM. Furthermore, the impacts of new physics on the top quark couplings are considered to be larger than that on any other fermions, and conflicts with the SM expectations could be measured as described in [1]. A search for rare decays of the top quark is one of such studies. The search for the top quark anomalous interactions via Flavour Changing Neutral Currents (FCNC) is of special interest. For the top quark, FCNC decays  $t \rightarrow q\gamma$  ( $q = u, c$ ) can not be seen at the tree level of the SM. These decays can only make loop contributions. As a result, the branching ratios of  $t \rightarrow q\gamma$  are very small, and they are at the order of  $10^{-10}$  [2–4]. However, various extensions of the SM, such as the quark-singlet model [5–7], the two-Higgs doublet model [8–13], the minimal supersymmetric model [14–20], supersymmetry [21], the top-color-assisted technicolor model [22] or extra dimension model [23, 24] could lead to a huge enrichment of those kind of decays.

The CDF collaboration bounds on the branching ratios at 95% C. L. for the process  $t \rightarrow q\gamma$  as follows [25]

$$BR(t \rightarrow u\gamma) + BR(t \rightarrow c\gamma) < 3.2\%. \quad (1)$$

Furthermore, the ZEUS collaboration obtained upper limits at 95% C.L. on the anomalous  $tq\gamma$  couplings  $\kappa_{tu\gamma} < 0.12$  [26]. The Large Hadron Collider (LHC) can produce large numbers of the top quark. Therefore, top quark interactions can be examined with high sensitivity. In particular, the ATLAS collaboration has been predicted as  $BR(t \rightarrow q\gamma) \sim 10^{-4}$  at  $5\sigma$  level [27].

The FCNC effective Lagrangian among the top quark, two quarks  $u, c$  and the photon  $\gamma$  can be written as [26]

$$L = \sum_{q_i=u,c} g_e e_t \bar{t} \frac{i\sigma_{\mu\nu} p^\nu}{\Lambda} \kappa_{tq_i\gamma} q_i A^\mu. \quad (2)$$

Here  $\kappa_{tq_i\gamma}$  is the anomalous coupling for the neutral currents with a photon;  $\Lambda$  is a new physics scale;  $\sigma_{\mu\nu} = [\gamma_\mu, \gamma_\nu]/2$ ;  $g_e$  is the electromagnetic coupling constant;  $e_t$  is the electric

charge of the top quark.  $\Lambda$  is the conventionally taken mass of the top quark ( $m_t$ ) for the sake of definiteness. Hence, we take  $\Lambda = m_t$ . Also, we assume in our calculations  $\kappa_{tu\gamma} = \kappa_{tc\gamma}$ . Using the anomalous interaction given in Eq.2, the decay width can be obtained as follows,

$$\Gamma(t \rightarrow q\gamma) = \frac{g_e^2 e_t^2 \kappa_{tq\gamma}^2 m_t^3}{8\pi\Lambda^2} \quad (q = u, c) \quad (3)$$

where we put the masses of the u and c quarks equal to the zero. Branching ratio of the anomalous  $t \rightarrow q\gamma$  decay can be given by the following equation, since the main decay mode of the top quark is  $t \rightarrow bW$

$$BR(t \rightarrow q\gamma) = \frac{\Gamma(t \rightarrow q\gamma)}{\Gamma(t \rightarrow bW)}. \quad (4)$$

Using this equation, from the experimental constraints of the CDF collaboration it is easy to obtain the magnitudes of the upper limits on  $\kappa_{tq\gamma} = 0.29$ .

In this work, we have examined anomalous FCNC interactions for the process  $pp \rightarrow p\gamma p \rightarrow pbWX$  at the LHC. We show a schematic diagram for the this reaction in Fig.1. The subprocess of the main reaction is  $\gamma q \rightarrow Wb$ . This process is becoming interesting as an additional way to investigate for SM or new physics.

In many situations, ultraperipheral collisions and elastic interactions can not be detected at the central detectors. Forward detectors are developed by the ATLAS and CMS collaborations to detect the scattering particles which can not be caught by the central detectors with limited pseudorapidity. These extra detectors are placed at distance of 220 m - 420 m from the central detectors. Usual  $pp$  deep inelastic scattering (DIS) incoming protons dissociate into partons. Therefore, DIS interactions have very sophisticated backgrounds. In the DIS process, made up of jets from the proton remnants, some ambiguities are created which make it hard to detect the new physics signals beyond the SM. However,  $\gamma\gamma$  or  $\gamma p$  interactions have a clean environment compared to the usual proton-proton DIS, since in  $\gamma\gamma$  or  $\gamma p$  collisions with almost real photons, a proton is emitted, while the photons remains intact. Because of both of the incoming protons remaining intact,  $\gamma\gamma$  collisions provide fewer backgrounds compared to the other processes. However,  $\gamma p$  collisions have higher energy and effective luminosity with respect to  $\gamma\gamma$  interactions.

In  $\gamma p$  collisions, the almost real photons with low virtuality are emitted from protons and it is a good approximation to assume that they are on-mass-shell. Because of the low

virtuality of the photons, the structure of the protons are not spoilt. Also, almost real photons are scattered with small angles, and then they have a low transverse momentum. Therefore, intact protons which are emitted photons deflect slightly their path along the beam pipe, and, generally, they can not be detected in central detectors. One of the main properties of forward detectors is to detect the intact protons with some momentum fraction loss given the formula,  $\xi = (|\vec{p}| - |\vec{p}'|)/|\vec{p}|$ , where  $\vec{p}$  and  $\vec{p}'$  are momentums of incoming protons and intact scattered protons, respectively. If the forward detectors are established closer to central detectors, a higher  $\xi$  can be obtained. Forward detectors can detect intact outgoing protons in the interval  $\xi_{min} < \xi < \xi_{max}$ . This interval is known as the acceptance of the forward detectors. ATLAS forward detectors have an acceptance of  $0.0015 < \xi < 0.15$  [28] and CMS-TOTEM forward detectors are placed closer to the central detectors and the acceptances span  $0.0015 < \xi < 0.5$ ,  $0.1 < \xi < 0.5$  [29, 30].

Photon-induced reactions in hadron collider phenomena were recently observed in the measurements of the CDF collaboration [31–37], and these measurements are consistent in both theoretical expectations with  $p\bar{p} \rightarrow p\ell^+\ell^-\bar{p}$  through two photon exchange ( $\gamma\gamma \rightarrow \ell^+\ell^-$ ). Therefore, the photon-induced interactions' potential at the LHC is significant, with its high energetic pp collisions, and high luminosity [28–30, 38–58]. Moreover, two photon reactions  $pp \rightarrow p\gamma\gamma p \rightarrow p\mu^+\mu^-p$ ,  $pp \rightarrow p\gamma\gamma p \rightarrow pe^+e^-p$ , and  $pp \rightarrow p\gamma\gamma p \rightarrow pW^+W^-p$  have been measured by the CMS collaboration from the early LHC data at  $\sqrt{s} = 7$  TeV [59–61].

The photon-induced reactions in  $pp$  collisions can be obtained in the framework of the equivalent photon approximation (EPA) [62, 63]. In this approximation the equivalent photon spectrum, given the virtuality  $Q^2$  and the energy of the quasi-real photons  $E_\gamma$  ( $E_\gamma \gg Q^2$ ), is given as follows:

$$\frac{dN}{dE_\gamma dQ^2} = \frac{\alpha}{\pi} \frac{1}{E_\gamma Q^2} \left[ \left(1 - \frac{E_\gamma}{E}\right) \left(1 - \frac{Q_{min}^2}{Q^2}\right) F_E + \frac{E_\gamma^2}{2E^2} F_M \right] \quad (5)$$

where  $E$  is the incoming proton energy ( $E_\gamma = \xi E$ ) and  $m_p$  is the mass of the proton. The remaining terms are as follows,

$$Q_{min}^2 = \frac{m_p^2 E_\gamma^2}{E(E - E_\gamma)}, \quad F_E = \frac{4m_p^2 G_E^2 + Q^2 G_M^2}{4m_p^2 + Q^2} \quad (6)$$

$$G_E^2 = \frac{G_M^2}{\mu_p^2} = \left(1 + \frac{Q^2}{Q_0^2}\right)^{-4}, \quad F_M = G_M^2, \quad Q_0^2 = 0.71 \text{ GeV}^2. \quad (7)$$

Here,  $F_E$  and  $F_M$  are functions of the electric and magnetic form factors respectively, and  $\mu_p^2 = 7.78$  is the magnetic moment of the proton. The cross section for the main process  $pp \rightarrow p\gamma p \rightarrow pWbX$  can be found by integrating  $\gamma q \rightarrow Wb$  subprocess cross section over the photon and quark spectra:

$$\begin{aligned} \sigma(pp \rightarrow p\gamma p \rightarrow pWbX) &= \sum_{q=u,c} \int_{Q_{min}^2}^{Q_{max}^2} dQ^2 \int_{x_{1min}}^{x_{1max}} dx_1 \\ &\times \int_{x_{2min}}^{x_{2max}} dx_2 \left( \frac{dN_\gamma}{dx_1 dQ^2} \right) \left( \frac{dN_q}{dx_2} \right) \hat{\sigma}_{\gamma q \rightarrow Wb}(\hat{s}). \end{aligned} \quad (8)$$

Here we have taken the  $Q_{max}^2 = 2 \text{ GeV}^2$  since  $Q_{max}^2$  greater than  $2 \text{ GeV}^2$  does not make a significant contribution to this integral. From Eq.8 the following equation can be obtained,

$$\begin{aligned} \sigma(pp \rightarrow p\gamma p \rightarrow pWbX) &= \sum_{q=u,c} \int_{Q_{min}^2}^{Q_{max}^2} dQ^2 \int_{\frac{M_{inv}}{\sqrt{s}}}^{\sqrt{\xi_{max}}} dz 2z \\ &\times \int_{MAX(z^2, \xi_{min})}^{\xi_{max}} \frac{dx_1}{x_1} \frac{dN_\gamma}{dx_1 dQ^2} N_q \left( \frac{z^2}{x_1} \right) \hat{\sigma}_{\gamma q \rightarrow Wb}(\hat{s}) \end{aligned} \quad (9)$$

where  $x_1$  is the ratio between scattered quasi-real photons and incoming proton energy  $x_1 = E_\gamma/E$  and  $x_2$  is the momentum fraction of the proton's momentum carried by the quark.  $\frac{dN_q}{dx_2}$  is the quark distribution function of the proton,  $\hat{s} = z^2 s$  and  $z = x_1 x_2$ .  $M_{inv}$  is total mass of the final state particles of the  $\gamma q \rightarrow Wb$  subprocess. In our paper, we have used Martin, Stirling, Thorne and Watt parton distribution functions [64]. During calculations, we have taken the quark virtuality  $Q'^2 = m_t^2$ . In all the results presented in this work, we impose a cut of pseudorapidity  $|\eta| < 2.5$  for final state particles from subprocess  $\gamma q \rightarrow Wb$  since central detectors of the ATLAS and CMS have a pseudorapidity  $|\eta|$  coverage of 2.5.

## II. PHENOMENOLOGICAL ANALYSIS

The subprocess  $\gamma q \rightarrow Wb$  consists of  $s$ ,  $t$  and  $u$  channel tree-level SM diagrams. Additionally, there is a one tree-level Feynman diagram an containing anomalous  $tq\gamma$  coupling in Fig.2. The total polarization summed amplitude square which consists of SM, new physics

and interference parts has been obtained in functions of the Mandelstam invariants  $\hat{s}$ ,  $\hat{t}$  and  $\hat{u}$  as follows,

$$|M_1|^2 = -\frac{g_e^2 g_w^2 V_{bq}^2 e_u^2}{m_w^2 s} (m_w^4 - (\hat{s} - \hat{t} + \hat{u})m_w^2 + (\hat{s} - m_b^2)\hat{u}), \quad (10)$$

$$|M_2|^2 = \frac{g_e^2 g_w^2 V_{bq}^2 e_b^2}{m_w^2 (\hat{t} - m_b^2)^2} (-2\hat{t}m_b^4 + (5m_w^4 + (\hat{s} - 5\hat{t} - \hat{u})m_w^2 + \hat{t}(2\hat{s} + 3\hat{u}))m_b^2 + \hat{t}(-m_w^4 + (-\hat{s} + \hat{t} + \hat{u})m_w^2 - \hat{t}\hat{u})), \quad (11)$$

$$|M_3|^2 = \frac{g_e^2 g_w^2 V_{bq}^2}{4m_w^4 (\hat{u} - m_w^2)^2} ((m_w^2 - \hat{u})(3m_w^2 - \hat{u})(m_b^2 + m_w^2 - \hat{t} - \hat{u})(\hat{u} - \hat{t}) + s(-3m_w^6 + (3\hat{s} - 14\hat{t} + 4\hat{u})m_w^4 - \hat{u}(4(\hat{s} + \hat{t}) + \hat{u})m_w^2 + (\hat{s} + 2\hat{t})\hat{u}^2 + m_b^2(11m_w^2 - 3\hat{u})(m_w^2 + \hat{u}))), \quad (12)$$

$$|M_4|^2 = \frac{g_e^2 g_w^2 \kappa_{tq\gamma}^2 e_t^2 V_{tb}^2}{m_w^2 \Lambda^2 ((\hat{s} - m_t^2)^2 + \Gamma_t^2 m_t^2)} \hat{s}((-m_w^4 + (\hat{s} - \hat{t} + \hat{u})m_w^2 + (m_b^2 - \hat{s})\hat{u})m_t^2 + \hat{s}(-m_w^4 + (\hat{s} + \hat{t} - \hat{u})m_w^2 + (m_b^2 - \hat{s})\hat{t})), \quad (13)$$

$$2Re(M_1^\dagger M_2) = \frac{g_e^2 g_w^2 V_{bq}^2 e_u e_b}{m_w^2 \hat{s}(\hat{t} - m_b^2)} ((\hat{s} - 3\hat{t} - \hat{u})m_b^4 + (4m_w^4 + (\hat{s} - \hat{t} + \hat{u})m_w^2 - 2\hat{s}^2 + \hat{u}^2 + 4\hat{s}\hat{t} + \hat{s}\hat{u} + 3\hat{t}\hat{u})m_b^2 - (m_w^2 - \hat{s} - \hat{t})(\hat{s} - \hat{t})^2 - (\hat{s} + \hat{t})\hat{u}^2 + (-4m_w^4 + (\hat{s} + \hat{t})m_w^2 - 2\hat{s}\hat{t})\hat{u}), \quad (14)$$

$$\begin{aligned}
2Re(M_1^\dagger M_3) = & \frac{g_e^2 g_w^2 V_{bq}^2 e_u}{4m_w^4 \hat{s}(m_w^2 - \hat{u})} (2(\hat{s} + 4\hat{t} - 4\hat{u})m_w^6 + (\hat{s}^2 + 13\hat{t}\hat{s} - 7\hat{u}\hat{s} - 12\hat{t}^2 + 12\hat{u}^2)m_w^4 + \\
& (-3\hat{s}^3 + (\hat{u} - 6\hat{t})\hat{s}^2 + (-3\hat{t}^2 - 3\hat{u}\hat{t} + 2\hat{u}^2)\hat{s} + 4(\hat{t} - \hat{u})(\hat{t} + \hat{u})^2)m_w^2 + \\
& \hat{s}\hat{u}(\hat{s} + \hat{t} - \hat{u})(\hat{s} + \hat{t} + \hat{u}) + m_b^2(-4(\hat{s} - 2\hat{t} + 2\hat{u})m_w^4 + (7\hat{s}^2 + 5\hat{t}\hat{s} - 3\hat{u}\hat{s} \\
& - 4\hat{t}^2 + 4\hat{u}^2)m_w^2 + \hat{s}\hat{u}(-\hat{s} - 3\hat{t} + \hat{u})),
\end{aligned} \tag{15}$$

$$2Re(M_1^\dagger M_4) = \frac{m_t e_u g_e^2 g_w^2 \kappa_{tq\gamma} e_t V_{bq} V_{tb} (m_t^2 - \hat{s})}{\Lambda m_w^2 ((\hat{s} - m_t^2)^2 + \Gamma_t^2 m_t^2)} (-3m_w^4 + (3\hat{s} - \hat{t} + \hat{u})m_w^2 + (m_b^2 - \hat{s})(\hat{t} + 2\hat{u})), \tag{16}$$

$$\begin{aligned}
2Re(M_2^\dagger M_3) = & \frac{g_e^2 g_w^2 V_{bq}^2 e_b}{4m_w^4 (\hat{u} - m_w^2)(\hat{t} - m_b^2)} (2(4\hat{s} + \hat{t} - 4\hat{u})m_w^6 + \\
& (-12\hat{s}^2 + 13\hat{t}\hat{s} + (\hat{t} - 4\hat{u})(\hat{t} - 3\hat{u}))m_w^4 + (4\hat{s}^3 + (4\hat{u} - 3\hat{t})\hat{s}^2 - (6\hat{t}^2 + \\
& 3\hat{u}\hat{t} + 4\hat{u}^2)\hat{s} - 3\hat{t}^3 - 4\hat{u}^3 + 2\hat{t}\hat{u}^2 + \hat{t}^2\hat{u})m_w^2 + \hat{t}\hat{u}(s + t - u)(s + t + u) + \\
& m_b^2(6m_w^6 - (21\hat{s} + \hat{t} + 9\hat{u})m_w^4 + (-5\hat{s}^2 + 13\hat{t}\hat{s} + 3\hat{u}\hat{s} + 8\hat{t}^2 + 6\hat{u}^2)m_w^2 + \\
& \hat{u}(-\hat{s}^2 - 3\hat{t}\hat{s} - 4\hat{t}^2 + \hat{u}^2 + \hat{t}\hat{u})) + m_b^4(4m_w^4 - (3\hat{s} + 5(\hat{t} + \hat{u}))m_w^2 + \\
& (\hat{s} + 3\hat{t} - \hat{u})\hat{u}))
\end{aligned} \tag{17}$$

$$\begin{aligned}
2Re(M_2^\dagger M_4) = & \frac{m_t e_b g_e^2 g_w^2 \kappa_{tq\gamma} e_t V_{bq} V_{tb}}{\Lambda m_w^2 (\hat{t} - m_b^2)((\hat{s} - m_t^2)^2 + \Gamma_t^2 m_t^2)} ((m_t^2 - \hat{s})(\hat{s} - \hat{u})m_b^4 + \\
& (m_w^4 + (3\hat{s} + \hat{t} - \hat{u})m_w^2 - 2\hat{s}^2 + \hat{u}^2 + \hat{s}\hat{u})m_b^2 + (m_w^2 - \hat{s})\hat{u}^2 + \\
& (m_w^2 - \hat{s})^2 s - m_w^2(m_w^2 - \hat{s} + \hat{t})\hat{u}) + 4\Gamma_t m_t(m_b^2 + m_w^2 - \hat{s})\epsilon^{p_1 p_2 p_3 p_4}),
\end{aligned} \tag{18}$$

$$\begin{aligned}
2Re(M_3^\dagger M_4) = & \frac{m_t g_e^2 g_w^2 \kappa_{tq\gamma} e_t V_{bq} V_{tb}}{2\Lambda m_w^2 (\hat{u} - m_w^2)((\hat{s} - m_t^2)^2 + \Gamma_t^2 m_t^2)} ((m_t^2 - \hat{s})\hat{s}(-m_w^4 + \\
& (\hat{s} - 8\hat{t} + \hat{u})m_w^2 - \hat{s}\hat{u} + m_b^2(7m_w^2 + \hat{u})) + (m_w^2 - \hat{u}) \\
& (4\Gamma_t m_t \epsilon^{p_1 p_2 p_3 p_4} - (m_t^2 - \hat{s})(m_b^2 + m_w^2 - \hat{t} - \hat{u})(\hat{t} - \hat{u}))),
\end{aligned} \tag{19}$$

where  $g_e$  and  $g_w$  are the electromagnetic and weak coupling constants,  $m_b$  is the  $b$  quark mass and  $m_w$  is the  $W$  boson mass.  $p_1, p_2, p_3$  and  $p_4$  are the momentums of the photon, incoming quark,  $W$  boson and  $b$  quark, respectively.  $V_{bq}$  and  $V_{tb}$  are the corresponding CKM matrix elements.  $e_u(e_b)$  is the electric charge of the  $u(b)$  quark. Also,  $\Gamma_t$  is the total decay width of the top quark. We have neglected the mass of the incoming quarks. In our calculations, it is assumed that the center of mass energy of the LHC is 14 TeV.

The total cross sections as a function of  $\kappa_{tq\gamma}$  for three acceptance regions  $0.0015 < \xi < 0.5$ ,  $0.0015 < \xi < 0.15$  and  $0.1 < \xi < 0.5$  are presented in Fig.3. We see from this figure that total cross sections for the  $0.0015 < \xi < 0.5$  and  $0.0015 < \xi < 0.15$  are close to each other. However, the cross section for  $0.1 < \xi < 0.5$  is rather smaller than the others. In Figs. 4a, 4b, 4c, we have plotted the SM and total cross sections of  $pp \rightarrow pWbX$  as functions of the transverse momentum cut ( $p_t$  cut or  $p_{t,min}$ ) of the final state particles for  $\kappa_{tq\gamma} = 0.01$  and three forward detectors acceptance regions:  $0.0015 < \xi < 0.5$ ,  $0.0015 < \xi < 0.15$  and  $0.1 < \xi < 0.5$ . As seen from the figures, in actual experiments both angular distribution and the  $p_t$  cut can be used to improve the sensitivity bounds since contributions of the new physics and the SM are well separated from each other for high  $p_t$  cut regions. Moreover, the acceptance region  $0.1 < \xi < 0.5$  has almost the same features as the other acceptance regions with a high  $p_t$  cut. It can be concluded that a high lower bound of the acceptance region mimics an extra  $p_t$  cut. Therefore, in this paper we estimate sensitivity of the  $pp \rightarrow p\gamma p \rightarrow pWbX$  process to be  $tq\gamma$  anomalous couplings using two different statistical analysis methods. First, we use a Poisson distribution, which is the appropriate sensitivity analysis since the number of SM events with these cuts are small enough. In this statistical analysis, the number of observed events are assumed to be equal to the SM prediction  $N_{obs} = S \times E \times BR \times L \times \sigma_{SM} = N_{SM}$ . Here  $S$  is the survival probability factor,  $E$  is the jet reconstruction efficiency and  $L$  is the integrated luminosity. We have taken a survival probability factor of  $S = 0.7$ , and jet reconstruction efficiency of  $E = 0.6$ . We consider  $W$  boson decay leptonically, hence here  $BR$  is the branching ratio of  $W$  boson to leptons. In the second statistical analysis we have used the  $\chi^2$  criterion without a systematic error which is given by

$$\chi^2 = \left( \frac{\sigma_{SM}^i - \sigma_{NEW}^i}{\sigma_{SM}^i \delta} \right)^2 \quad (20)$$

where  $\sigma_{NEW}$  is the total cross section including  $SM$  and new physics and  $\delta$  is the statistical



error. We show the sensitivity of the 95% C.L. parameter  $\kappa_{tq\gamma}$  as a function of integrated LHC luminosity for  $0.0015 < \xi < 0.5$ ,  $0.0015 < \xi < 0.15$ ,  $0.1 < \xi < 0.5$  in Figs.5a, 5b, 5c. We set  $p_t > 30$  GeV in these figures. As seen from the Fig.4, SM backgrounds could be smaller than 10 depending on the integrated luminosity. Therefore, in these kinematical regions we have used Poisson analysis for the  $N_{SM} < 10$  and, we have used  $\chi^2$  criterion for  $N_{SM} > 10$ . We understand from the figures that the best sensitivity has been obtained in the  $0.0015 < \xi < 0.5$  case. In Figs. 6a, 6b, 6c we show the 95% C.L. lower bounds for  $\kappa_{tq\gamma}$  as a function of integrated LHC luminosity for  $0.0015 < \xi < 0.5$ ,  $0.0015 < \xi < 0.15$ ,  $0.1 < \xi < 0.5$  and  $p_t > 500$  GeV. In this high  $p_t$  cut region, SM events smaller than 10 for all of the luminosity values as seen from the Fig.4. Hence, in Fig.6 we use only Poisson analysis. Fig.6 reflects similar behaviour to Fig.5. These figures show that the obtained sensitivity bounds in Fig.5 are better than in Fig.6. However, high  $p_t$  cut regions (Fig.4) have a very clean environment. Therefore, any signal which conflicts with the SM expectations would be a credible clue for there being something beyond the SM.

### III. CONCLUSIONS

By using very forward detectors, the LHC can be designed as a high energy photon-photon and photon-proton collider. There is no existing high energy photon-photon, photon-proton collider with this property. The process  $pp \rightarrow p\gamma p \rightarrow pWbX$  provides fewer backgrounds than the pure DIS process due to one of the incoming protons being intact after the collision. The detection of the intact protons in forward detectors make it possible to determine the momentum of the quasi-real photons. This situation may be useful in determining the kinematics of the process. Moreover, anomalous  $tq\gamma$  couplings might also be uniquely revealed in single top photoproduction [28].

In these motivations, we have analysed the potential of the  $pp \rightarrow p\gamma p \rightarrow pWbX$  at the LHC to probe anomalous  $tq\gamma$  couplings for three forward detector acceptances  $0.0015 < \xi < 0.5$ ,  $0.0015 < \xi < 0.15$  and,  $0.1 < \xi < 0.5$ . We determined that this photon-induced process has an important potential to examine anomalous  $tq\gamma$  couplings. We have investigated the sensitivity bounds for  $p_t > 30$  GeV and  $p_t > 500$  GeV regions. The results we obtained improve the sensitivity bounds on  $tq\gamma$  couplings by up to a factor of 116 for  $p_t > 30$  GeV with respect to current experimental data [25] as seen from the Fig.5a. Furthermore, for

$p_t > 500$  GeV, the results improve the sensitivity bounds on  $tq\gamma$  couplings by up to a factor of 38. Moreover, these high  $p_t$  cut regions can give extra opportunities to search for new physics with very low backgrounds. As a result, forward detectors provide an enhancement of the physics studied at the LHC.

- 
- [1] J. A. Aguilar-Saavedra, Nucl. Phys. B **812**, 181 (2009).
  - [2] B. Grzadkowski, J. F. Gunion and P. Krawczyk, Phys. Lett. B **268** 106 (1991).
  - [3] G. Eilam, J. L. Hewett and A. Soni, Phys. Rev. D **44** 1473 (1991).
  - [4] G. Couture, C. Hamzaoui and H. Knig, Phys. Rev. D **52** 1713 (1995).
  - [5] J. A. Aguilar-Saavedra and B. M. Nobre, Phys. Lett. B **553** 251(2003).
  - [6] F. del Aguila, J. A. Aguilar-Saavedra and R. Miquel, Phys. Rev. Lett. **82** 1628 (1999).
  - [7] J. A. Aguilar-Saavedra, Phys. Rev. D **67** 035003 (2003). Erratum-ibid. D **69** 099901 (2004).
  - [8] T. P. Cheng and M. Sher, Phys. Rev. D **35** 3484 (1987).
  - [9] B. Grzadkowski, J. F. Gunion and P. Krawczyk, Phys. Lett. B **268** 106 (1991).
  - [10] M. E. Luke and M. J. Savage, Phys. Lett. B **307** 387 (1993).
  - [11] D. Atwood, L. Reina and A. Soni, Phys. Rev. D **53** 1199 (1996).
  - [12] D. Atwood, L. Reina and A. Soni, Phys. Rev. D **55** 3156 (1997).
  - [13] S. Bejar, J. Guasch and J. Sola, Nucl. Phys. B **600** 21 (2001).
  - [14] C. S. Li, R. J. Oakes and J. M. Yang, Phys. Rev. D **49** 293 (1994). Erratum-ibid.D **56**:3156,(1997).
  - [15] G. M. de Divitiis, R. Petronzio and L. Silvestrini, Nucl. Phys. B **504** 45 (1997).
  - [16] J. L. Lopez, D. V. Nanopoulos and R. Rangarajan, Phys. Rev. D **56** 3100 (1997).
  - [17] J. Guasch and J. Sola, Nucl. Phys. B **562** 3 (1999).
  - [18] D. Delepine and S. Khalil, Phys. Lett. B **599** 62 (2004).
  - [19] J. J. Liu, C. S. Li, L. L. Yang and L. G. Jin, Phys. Lett. B **599** 92 (2004).
  - [20] J. J. Cao et al., Phys. Rev. D **75** 075021 (2007).
  - [21] J. M. Yang, B.-L. Young and X. Zhang, Phys. Rev. D **58** 055001 (1998).
  - [22] G. Lu, F. Yin, X. Wang and L. Wan, Phys. Rev. D **68** 015002 (2003).
  - [23] G. P. K. Agashe and A. Soni, Phys. Rev.D **71** 016002 (2005).
  - [24] G. P. K. Agashe and A. Soni, Phys. Rev. D **75** 015002 (2007).
  - [25] F. Abe et al., (CDF Collaboration), Phys. Rev. Lett. **80** 2525-2530 (1998).
  - [26] ZEUS Collaboration, Phys. Lett. B, **708** 27-36 (2012).
  - [27] J. Carvalho et al., (ATLAS Collaboration), Eur. Phys. J. C **52** 999-1019 (2007).
  - [28] M. Albrow *et al.*, (FP420 R and D Collaboration), J. Instrum. **4**, T10001 (2009).

- [29] O. Kepka and C. Royon, Phys. Rev. D **78**, 073005 (2008).
- [30] V. Avati and K. Osterberg, Report No. CERN-TOTEM-NOTE-2005-002, (2006).
- [31] A. Abulencia *et al.*, (CDF Collaboration), Phys. Rev. Lett. **98**, 112001 (2007).
- [32] T. Aaltonen *et al.*, (CDF Collaboration), Phys. Rev. Lett. **99**, 242002 (2007).
- [33] T. Aaltonen *et al.*, (CDF Run II Collaboration), Phys. Rev. D **77**, 052004 (2008).
- [34] T. Aaltonen *et al.*, (CDF Collaboration), Phys. Rev. Lett. **102**, 242001 (2009).
- [35] T. Aaltonen *et al.*, (CDF Collaboration), Phys. Rev. Lett. **102**, 222002 (2009).
- [36] O. Kepka and C. Royon, Phys. Rev. D **76**, 034012 (2007).
- [37] M. Rangel, C. Royon, G. Alves, J. Barreto and R. Peschanski, Nucl. Phys. B **774**, 53 (2007).
- [38] V. Khoze, A. Martin, R. Orava and M. Ryskin, Eur. Phys. J. **C19**, 313 (2001).
- [39] M. Albrow, T. Coughlin and J. Forshaw, Prog. Part. Nucl. Phys. **65**, 149 (2010).
- [40] I. F. Ginzburg and A. Schiller, Phys. Rev. D **57**, 6599 (1998).
- [41] I. F. Ginzburg and A. Schiller, Phys. Rev. D **60**, 075016 (1998).
- [42] S. Lietti, A. Natale, C. Roldao and R. Rosenfeld, Phys. Lett. B **497**, 243 (2001).
- [43] K. Piotrkowski, Phys. Rev. D **63**, 071502(R) (2001).
- [44] V. Goncalves and M. Machado, Phys. Rev. D **75**, 031502(R) (2007).
- [45] M. Machado, Phys. Rev. D **78**, 034016 (2008).
- [46] S. Atağ, S. C. İnan and İ. Şahin, Phys. Rev. D **80**, 075009 (2009).
- [47] İ. Şahin and S. C. İnan, JHEP **09**, 069 (2009).
- [48] S. C. İnan, Phys. Rev. D **81**, 115002 (2010).
- [49] E. Chapon, C. Royon and O. Kepka, Phys. Rev. D **81**, 074003 (2010).
- [50] S. Atağ and A. Billur, JHEP **11** 060 (2010).
- [51] İ. Şahin and A. Billur, Phys. Rev. D **83**, 035011 (2011).
- [52] İ. Şahin and M. Köksal, JHEP **11**, 100 (2011).
- [53] S. C. İnan and A. Billur, Phys. Rev. D **84**, 095002 (2011).
- [54] R. S. Gupta, Phys. Rev. D **85**, 014006 (2012).
- [55] İ. Şahin, Phys. Rev. D **85**, 033002 (2012).
- [56] L. N. Epele *et al.*, Eur. Phys. J. Plus **127**, 60 (2012).
- [57] İ. Şahin and B. Şahin, Phys. Rev. D **86**, 115001 (2012).
- [58] A. A. Billur, Europhys. Lett. **101**, 21001 (2013).
- [59] S. Chatrchyan *et al.*, (CMS Collaboration), JHEP **1201**, 052 (2012).

- [60] S. Chatrchyan *et al.*, (CMS Collaboration), JHEP **1211**, 080 (2012).
- [61] CMS Collaboration, JHEP **07**, 116 (2013).
- [62] V. Budnev, I. Ginzburg, G. Meledin and V. Serbo, Phys. Rep. **15**, 181 (1975).
- [63] G. Baur *et al.*, Phys. Rep. **364**, 359 (2002).
- [64] A. D. Martin *et al.*, Eur. Phys. J. C **63**, 189 (2009).

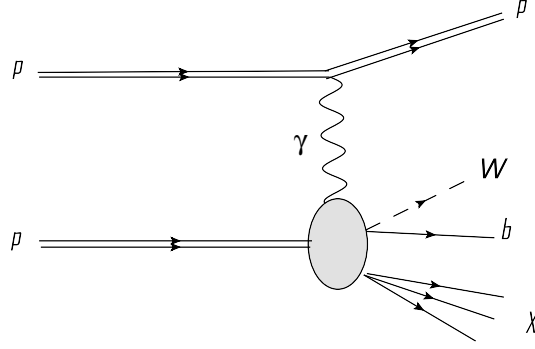


FIG. 1: Schematic diagram for the reaction  $pp \rightarrow p\gamma p \rightarrow pWbX$ .

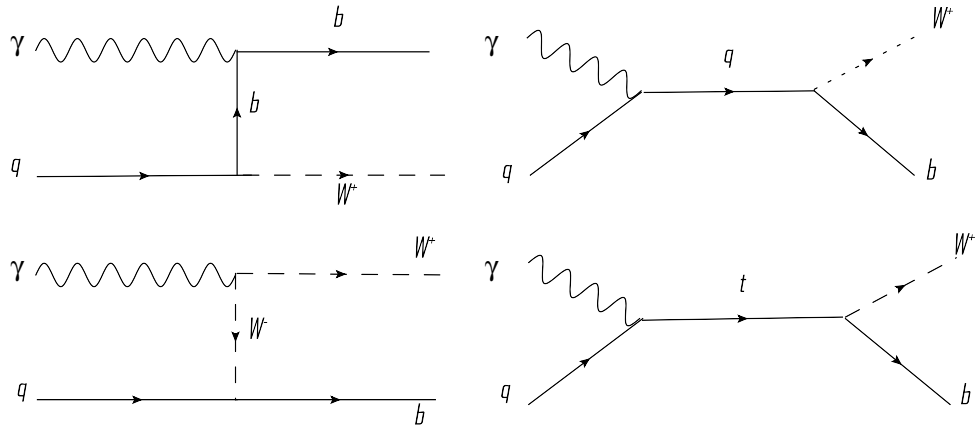


FIG. 2: Tree level Feynman diagrams for the subprocess  $\gamma q \rightarrow Wb$  ( $q = u, c$ ) in the presence of the anomalous  $tq\gamma$  couplings.

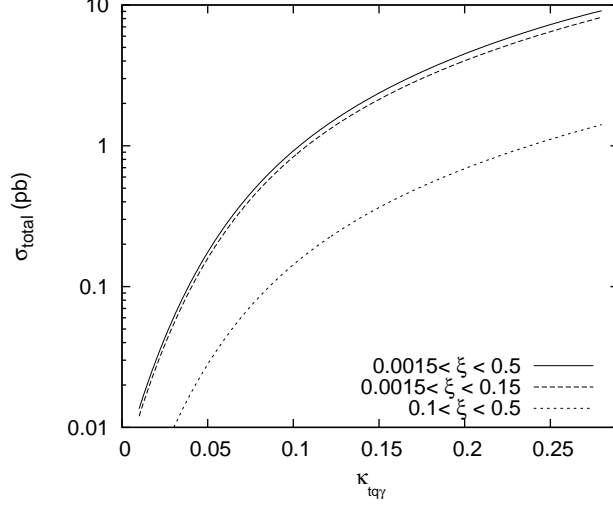


FIG. 3: The total cross sections of  $pp \rightarrow p\gamma p \rightarrow pWbX$  as a function of anomalous  $tq\gamma$  coupling ( $\kappa_{tq\gamma}$ ) for three different forward detector acceptances stated in the figure. It is assumed that the center of mass energy of the LHC is 14 TeV. Also, we impose cuts  $|\eta| < 2.5$  and  $p_t > 30$  GeV.

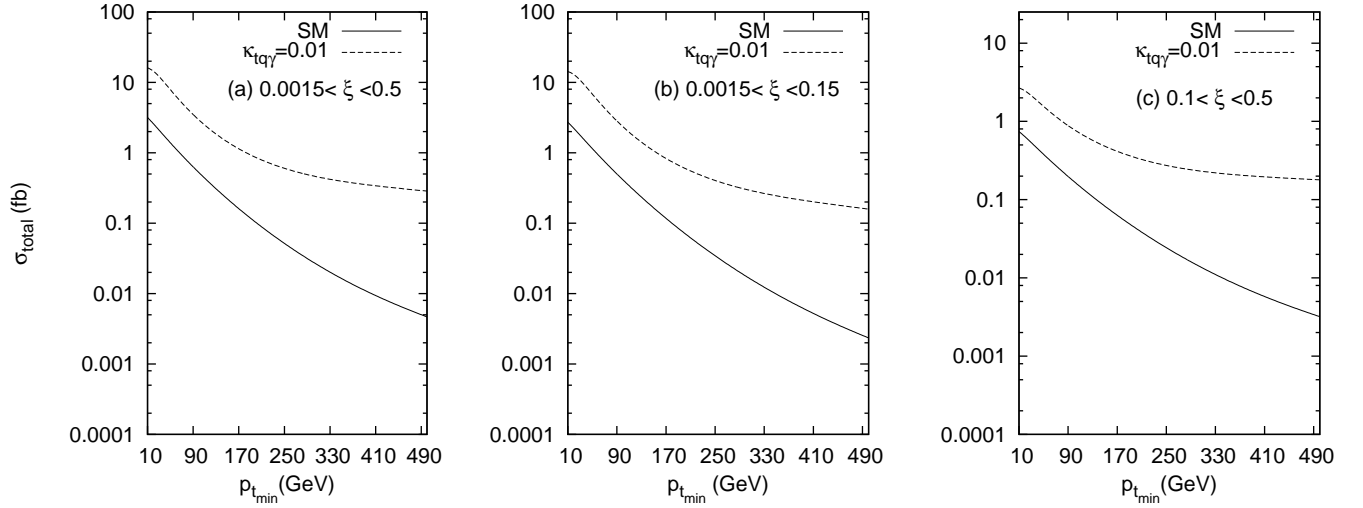


FIG. 4: Cross sections of  $pp \rightarrow p\gamma p \rightarrow pWbX$  as a function of the transverse momentum cut on the final state particles for three forward detector acceptances:  $0.0015 < \xi < 0.5$ ,  $0.0015 < \xi < 0.15$ , and  $0.1 < \xi < 0.5$ . Solid lines are for the SM and the dotted lines are for the total cross sections with  $\kappa_{tq\gamma} = 0.01$ . We impose cuts  $|\eta| < 2.5$  and  $p_t > 30$  GeV.

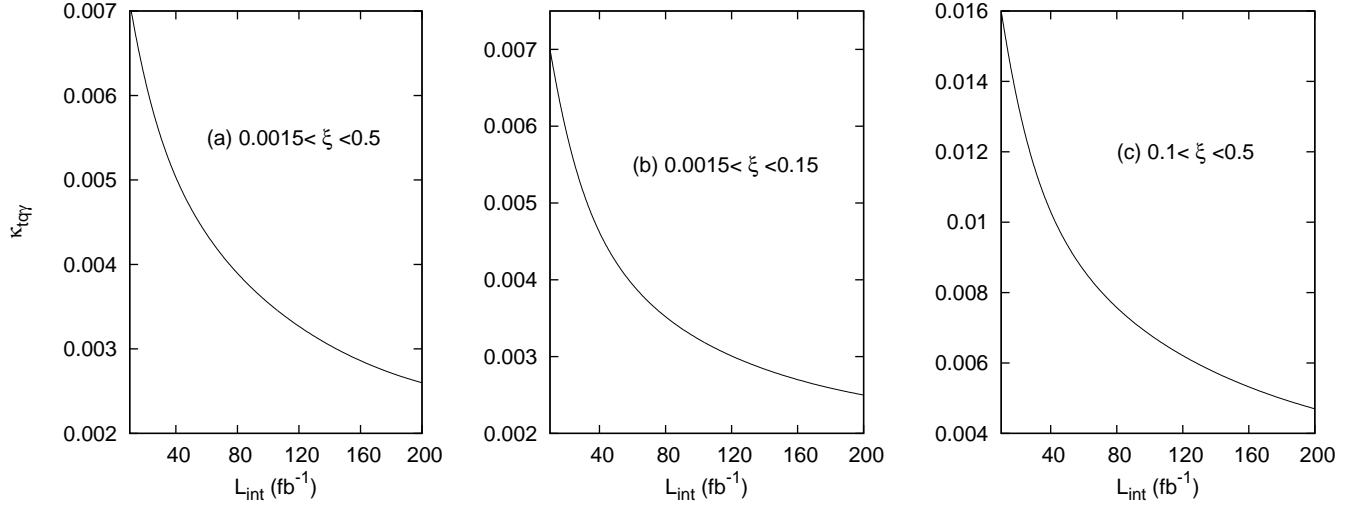


FIG. 5: 95% C.L. lower bounds for  $\kappa_{tq\gamma}$  as a function of integrated LHC luminosity for three forward detector acceptances:  $0.0015 < \xi < 0.5$ ,  $0.0015 < \xi < 0.15$  and,  $0.1 < \xi < 0.5$ . We impose the following cuts:  $p_t > 30$  GeV and  $|\eta| < 2.5$ .



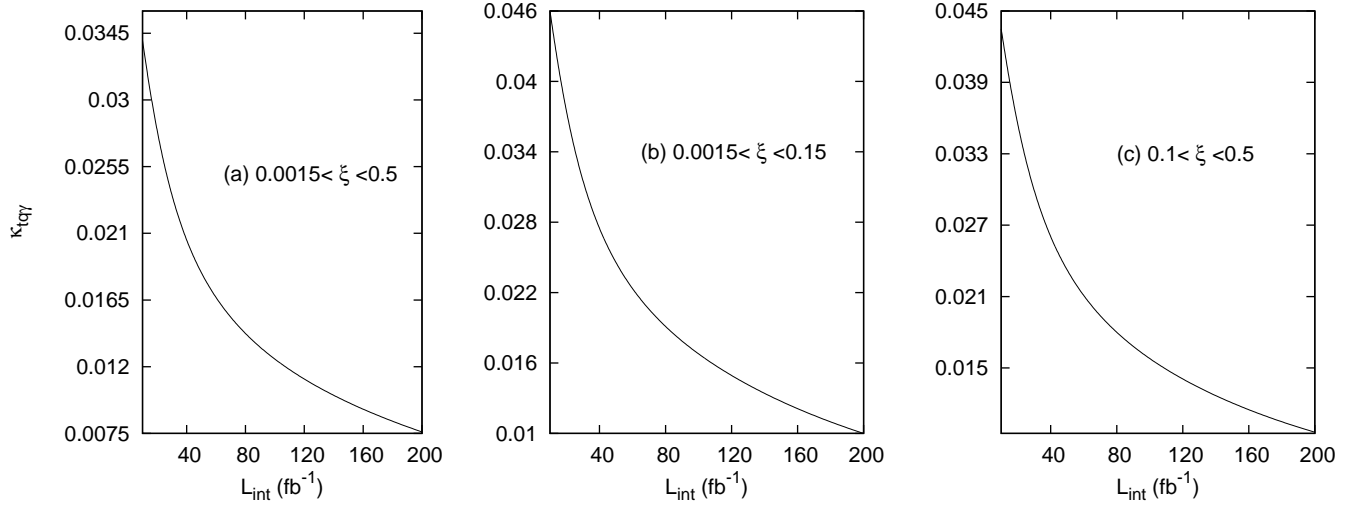


FIG. 6: 95% C.L. lower bounds for  $\kappa_{tq\gamma}$  as a function of integrated LHC luminosity for three forward detector acceptances:  $0.0015 < \xi < 0.5$ ,  $0.0015 < \xi < 0.15$  and,  $0.1 < \xi < 0.5$ . We impose the following cuts:  $p_t > 500$  GeV and  $|\eta| < 2.5$ .